Kinetic Studies of Drug–Dinucleotide Complexes†

Pari Davanloo and Donald M. Crothers*

ABSTRACT: Three classes of kinetic behavior are observed in the complexes of actinomycin or ethidium with deoxydinucleotides. First, the initial dinucleotide binding to form a 1:1 complex is a rapid bimolecular process, whose rate could be measured for combination of actinomycin with d(pTpG), d(pGpT), d(pGpA), d(pApG), d(pGpG), and d(pCpG) and for combination of ethidium with d(pGpC). Second, with one exception, all reactions in which a second dinucleotide is added to form a 2:1 dinucleotide–drug complex are limited by a first-order step at high concentration. This class includes the combination of actinomycin with all dinucleotides tested except d(pGpC), and the reaction of ethidium with nucleotides of complementary sequence pyrimidine–purine, such as d(pCpG). The final class is the special case of d(pGpC) interacting to form a 2:1 complex with actinomycin. Third-order kinetics is observed, with no evidence for a first-order, rate-limiting step.

Actinomycin and ethidium bromide are two important drugs whose functions are of considerable biochemical interest. Actinomycin binds strongly to double-stranded DNA (but not to double-stranded RNA) and inhibits enzymatic DNA-dependent RNA synthesis (Kirk, 1960; Kersten et al., 1960). Ethidium bromide binds to DNA and RNA; it inhibits DNA synthesis in vivo (Henderson, 1963) and interferes with DNA-dependent DNA and RNA polymerases in vitro (Elliot, 1963; Waring, 1964). The interactions of these drugs with DNA and RNA have been the subjects of extensive investigation. Fuller and Waring (1964) proposed that ethidium intercalates between the base pairs of DNA, a type of binding first proposed by Lerman (1961) for an acridine derivative. Tsai et al. (1975) recently solved the three-dimensional structure of EBr-5-iodoUpA to atomic resolution by x-ray crystallography, visualizing directly the intercalative binding of EBr[1] to a fragment of a nucleic acid double helix for the first time. The detailed kinetic mechanism of binding of EBr to calf thymus DNA was reported by Bresloff and Crothers (1975). Their results revealed that EBr can directly transfer from one binding site to another as well as intercalate into DNA from the free state.

Based on the structure of a crystalline complex of actinomycin D and deoxyguanosine, Sobell and Jain (1971, 1972) proposed a detailed stereochemical model for the binding of AmD to DNA. This model suggests that the phenoxazone ring system on actinomycin intercalates between guanine-cystosine sequences in DNA and that the peptide side chains of the actinomycin molecule, which are located in the narrow groove of DNA helix, form hydrogen bonds to deoxyguanosines. The intercalative model had earlier been proposed by Müller and Crothers (1968) based on detailed spectroscopic, hydrodynamic, and kinetic measurements and was supported by observations reported by Waring (1970) and Wang (1971) that actinomycin is able to unwind supercoiled covalently closed circular DNA.

Recently, the complexation of actinomycin (Schara and Müller, 1972; Krugh, 1972; Krugh and Neely, 1973a,b; Davanloo and Crothers, 1976) and ethidium bromide (Kreishman et al., 1971; Krugh et al., 1975; Krugh and Reinhardt, 1975) to a series of dinucleotides of different sequences has been extensively studied in the hope that information obtained from studies of these simple model systems would help elucidate further the mode of binding of these drugs to nucleic acids. Krugh and Reinhardt (1975) have reported spectral titration, fluorescence, circular dichroism, and nuclear magnetic resonance spectroscopic studies of solution complexes of ethidium bromide with dinucleotides. Their results indicate that ethidium bromide displays a preference for binding to pyrimidine (3′,5′) purine sequence isomers. Their studies also provide more direct evidence for the intercalation model for complexes of EBr with dinucleotides in solution.

For further understanding of the binding of actinomycin and ethidium bromide to dinucleotides, we have turned our attention to mechanistic and kinetic aspects of these interactions. Using the temperature-jump relaxation technique, we observed three general classes of kinetic behavior for drug–dinucleotide complexes. First, 1:1 complexes are formed in a simple bimolecular reaction whose rate constant can approach the diffusion-controlled limit, and whose relaxation time is sometimes too fast for the conventional temperature-jump method. Second, with a single exception all complexes involving two nucleotide chains per drug molecule require a first-order rearrangement step which limits the rate at high concentration. This kinetic barrier couples with the bimolecular steps to produce a second relaxation time which can either increase or decrease with increasing concentration. We propose that the first-order step involves a rearrangement of the 1:1 drug–dinucleotide complex to accommodate a second dinucleotide. The third class of kinetic behavior has only one representative so far, namely, the complex of actinomycin with d(pGpC). In this case no evidence for rate limitation by rearrangement of an intermediate 1:1 actinomycin–d(pGpC) complex was found. Instead, the reaction shows a single relaxation time over the entire concentration range studied, following the third-order kinetic law expected for formation of the termolecular actinomycin–$[d(pGpC)]_2$ complex.

† From the Department of Chemistry, Yale University, New Haven, Connecticut 06520. *Received May 7, 1976.* Supported by Grant CA 15583 from the National Cancer Institute, United States Public Health Service.

[1] Abbreviations used: EBr, ethidium bromide; AmD, actinomycin D; dG, 2′-deoxyguanosine; dpG, 2′-deoxyguanosine 5′-phosphate; dGp, 2′-deoxyguanosine 3′-phosphate; BPES buffer, 0.008 M Na_2HPO_4, 0.02 M NaH_2PO_4, 0.18 M NaCl, 0.001 M Na_2EDTA; Na_2EDTA, disodium ethylenediaminetetraacetate; poly(U), poly(uridylic acid).

Materials and Methods

Materials. Ethidium bromide was purchased from Calbiochem. Actinomycin D (C_1) was a gift of Merck, Sharp and Dohme. Actinomycin C_3 was given to us by Dr. W. Müller. The deoxydinucleotides were purchased from Collaborative Research, Inc. 2′-Deoxyguanosine (dG), 2′-deoxyguanosine 5′-phosphate (dpG), and 2′-deoxyguanosine 3′-phosphate (dGp) were purchased from Sigma Chemical Co.

All experiments were performed on material dissolved in BPES buffer at pH 6.9 (0.008 M Na_2HPO_4, 0.02 M NaH_2PO_4, 0.18 M NaCl, 0.001 M Na_2EDTA). Stock solutions (50 mM) of deoxydinucleotides were prepared, and their concentrations were determined using the extinction coefficients given by Collaborative Research, Inc.

Kinetic Measurements. Relaxation-kinetic measurements were carried out using a temperature-jump instrument as previously described (Crothers, 1971). In each concentration-dependence study, the dinucleotide concentration varied but the total concentration of dye was kept constant.

Equilibrium sedimentation measurements of the ethidium bromide + d(pCpG) complex were done with a Spinco Model E analytical ultracentrifuge equipped with absorption optics. The molecular weight of such a multicomponent system can be calculated from the following equation (Tanford, 1961):

$$M_{\text{complex}} = \tfrac{1}{2}M_{\text{NaCl}}Z\left(\frac{1-\bar{V}_{\text{NaCl}}\rho}{1-\bar{V}_{\text{comp}}\rho}\right)+\frac{2RT\dfrac{\partial \ln C}{\partial r^2}}{(1-\bar{V}_{\text{comp}}\rho)\omega^2} \quad (1)$$

where Z is the charge on the complex (all phosphates were assumed singly ionized), $\bar{V}_{\text{comp}}$ the partial specific volume of complex, ρ the density of the buffer solution, and C the concentration of the complex at distance r from the axis of rotation.

If several species are present, each at molar concentration C_i with extinction coefficient ϵ_i, eq 1 can be solved for d ln C_i/dr^2, multiplied by $C_i\epsilon_i$, divided by $\Sigma\epsilon_iC_i$, summed over i and rearranged to give

$$\psi = \frac{\sum M_i\epsilon_iC_i(1-\bar{V}_i\rho)}{\sum\epsilon_iC_i} - \tfrac{1}{2}M_{\text{NaCl}}(1-\bar{V}_{\text{NaCl}}\rho)\frac{\sum\epsilon_iC_iZ_i}{\sum\epsilon_iC_i} \quad (2a)$$

where we define ψ to be

$$\psi = \frac{2RT}{\omega^2}\frac{d \ln A}{dr^2} \quad (2b)$$

A is the absorbance of the solution. The partial specific volumes needed in eq 2 were determined for EBr and d(pCpG) by equilibrium sedimentation on the isolated species, using eq 1 to calculate $\bar{V}$. We took $\bar{V}_{\text{NaCl}} = 0.3$, $\rho = 1.0094$ at $T = 281.2$ K. $\bar{V}$ for the 1:1 and 1:2 complexes was calculated by assuming additivity of the molar volumes of the components. Thus

$$\bar{V}_{\text{comp}} = \frac{nM_{\text{d(pCpG)}}\bar{V}_{\text{d(pCpG)}} + M_{\text{EBr}}\bar{V}_{\text{EBr}}}{nM_{\text{d(pCpG)}} + M_{\text{EBr}}}$$

where n is the number of moles of d(pCpG) per mole of EBr in the complex. ϵ values were estimated from the extinction of complexes of EBr with double- and single-stranded polynucleotides.

Melting Curves. The absorption-temperature profiles of the ethidium bromide + d(pCpG) complex were recorded on a Cary Model 14 spectrophotometer. Samples were placed in 0.1-cm path length, thermostated cuvettes (Helma). The transition was followed at λ 465 nm.

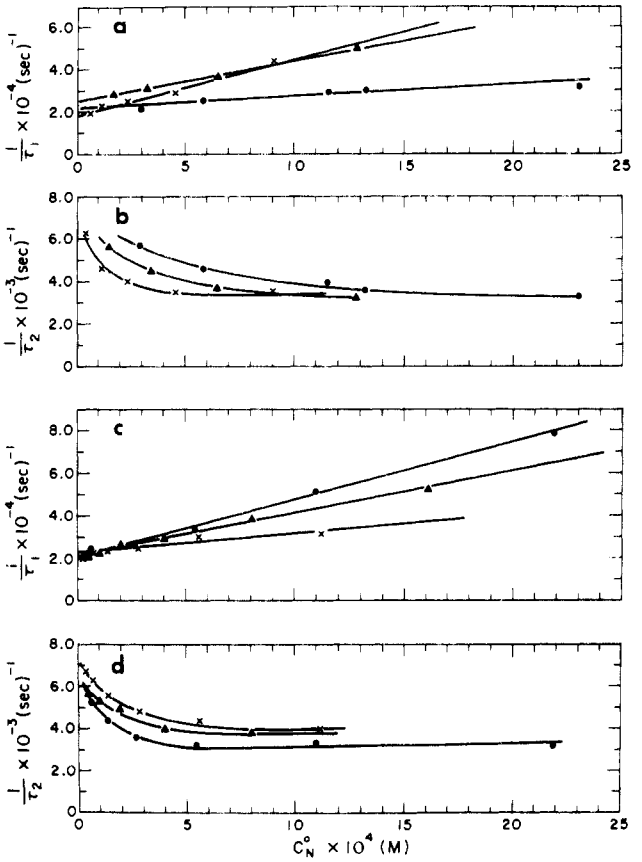

FIGURE 1: Concentration dependence of the two relaxation times, τ_1 and τ_2 for a series of deoxydinucleotides at $T = 7.4$ °C, $C_A^\circ = 0.04$ mM in BPES buffer. (a) Plot of $1/\tau_1$ vs. C_N°: (X) AmC_3-d(pGpG); (▲) AmC_3-d(pGpT); (●) AmC_3-d(pGpA). (b) Plot of $1/\tau_2$ vs. C_N°: (X) AmC_3-d(pGpG); (▲) AmC_3-d(pGpT); (●) AmC_3-d(pGpA). (c) Plot of $1/\tau_1$ vs. C_N°: (●) AmC_3-d(pApG); (▲) AmC_3-d(pTpG); (X) AmC_3-d(pCpG). (d) Plot of $1/\tau_2$ vs. C_N°. (●) AmC_3-d(pApG); (▲) AmC_3-d(pTpG); (X) AmC_3-d(pCpG).

CD Measurements. CD spectra for actinomycin–deoxydinucleotide complexes were recorded at 4 °C on a Cary 60 spectropolarimeter equipped with a 6001 CD attachment. The data are expressed as the directly measured ellipticity θ in degrees.

Results

Investigation of Complexation between Actinomycin C_3 and Some Deoxydinucleotides

Kinetic Studies. Relaxation kinetic experiments for dG, dpG, and dGp show a fast relaxation in the range of a few tens of microseconds, as originally reported by Müller and Spatz (1965). We confirmed that the concentration dependence of $1/\tau$ determined at λ 435 nm was linear with nucleotide concentration, with slope and intercept in approximate agreement with observed binding constants (Davanloo and Crothers, 1976).

Relaxation kinetic experiments for the binding of d(pGpT), d(pTpG), d(pGpA), d(pApG), d(pGpG), and d(pCpG) to AmC_3 show two well-separated relaxation times, usually differing by about a factor of six in time scale. The concentration dependence of the relaxation times in a series of experiments in which total AmC_3 concentration was held constant has been examined, and typical results are shown in Figure 1. We observed that the faster relaxation rate $1/\tau_1$ varies linearly with

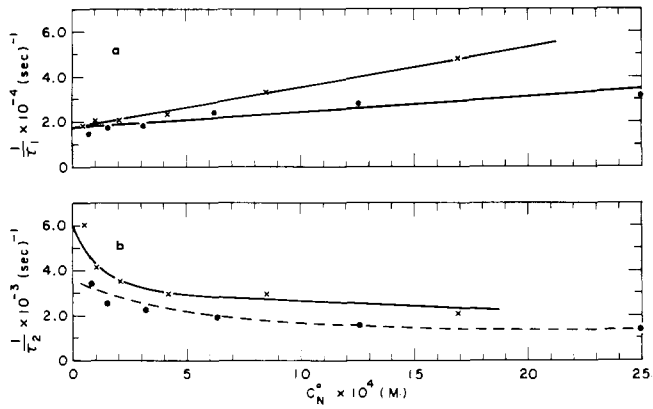

FIGURE 2: Comparison between actinomycin C_3 and actinomycin D (=C) binding to d(pApG) at T = 2 °C, C_A° = 0.04 mM in BPES buffer. (a) Plot of $1/\tau_1$ vs. C_N°; (X) AmC_3-d(pApG); (●) AmD-d(pApG). (b) Plot of $1/\tau_2$ vs. C_N°: (X) AmC_3-(pApG); (●) AmD-d(pApG); (- - -) theoretical curve calculated for AmD using the mechanism given in eq 8, and following rate constants, $k_{12} = 3 \times 10^7$ M^{-1} s^{-1}; $k_{21} = 1.4 \times 10^4$ s^{-1}; $k_{23} = 0.9 \times 10^3$ s^{-1}; $k_{32} = 4 \times 10^3$ s^{-1}; $k_{34} = k_{12} = 3 \times 10^7$ M^{-1} s^{-1}; $k_{32} = k_{21} = 1.4 \times 10^4$ s^{-1}.

dinucleotide concentration, but the slower rate $1/\tau_2$ shows an unusual concentration dependence (Figures 1b and d): as we decreased the dinucleotide concentration, τ_2 became faster. The slow relaxation rate $1/\tau_2$ is similar for all the nucleotides tested, both in the plateau value at high concentration and in the probable limiting value at low concentration. The actinomycin peptide rings have an effect on both the faster and slower relaxation rates, as shown by the data in Figure 2, comparing actinomycin C_3 with actinomycin D (= C_1). The slower relaxation for AMC_3 than for AmD is of interest in connection with the observation by Müller and Crothers (1968) that the dissociation rate of AmD from DNA (τ_3 = 1500 s) is slower than that of AmC_3 (τ_3 = 570 s).

Relaxation-kinetic experiments on the binding of d(pGpC) to AmC_3 reveal only a single relaxation time in the range of roughly 1 ms. We found that $1/\tau$ varied linearly with the square of the total dinucleotide concentration and, therefore, tested the third-order reaction mechanism

$$\text{Am} + 2\text{d(pGpC)} \underset{k_{21}}{\overset{k_{12}}{\rightleftharpoons}} \text{Am-[d(pGpC)]}_2$$

for which the relaxation time is given by

$$1/\tau = k_{12}(\bar{D}^2 + 4\bar{A}\bar{D}) + k_{21} \qquad (3)$$

where $\bar{A}$ and $\bar{D}$ are the equilibrium concentrations of actinomycin and dinucleotide, respectively. Figure 3 shows the data plotted according to this equation; we used the value of K from our earlier phase separation experiment (Davanloo and Crothers, 1976; $K = k_{12}/k_{21} = 6.7 \times 10^7$ M^{-2}) to calculate $\bar{A}$ and $\bar{D}$. From the slope and intercept of Figure 3, we estimate that $k_{12} = (2.7 \pm 0.5) \times 10^{10}$ M^{-2} s^{-1}, $k_{21} = (5 \pm 2) \times 10^2$ s^{-1}, $K = (5.4 \pm 2) \times 10^7$ M^{-2}.

The observed kinetic behavior is consistent with the cooperative binding of two d(pGpC) molecules to one actinomycin, forming a miniature double helix as reported previously (Schara and Müller, 1972; Krugh and Neely, 1973b; Davanloo and Crothers, 1976). d(pGpC) is the only dinucleotide which did not show a first-order (concentration independent) rate-determining step among those whose complex with actinomycin we investigated.

Circular Dichroism Studies. In Figure 4, CD spectra in the visible region of actinomycin C_3 and actinomycin C_3-deoxy-

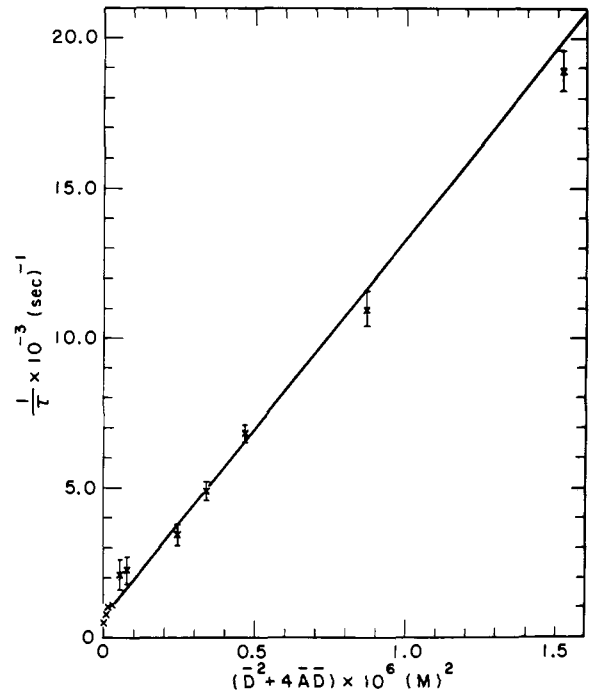

FIGURE 3: Reciprocal relaxation time vs. $\bar{D}^2 + 4\bar{A}\bar{D}$ for the AmC_3-d(pGpC) system in BPES buffer at T = 8 °C and C_A° = 0.04 mM.

dinucleotide complexes are shown. Actinomycin C_3 has a negative ellipticity band in the vicinity of 375 nm. The CD spectra of the AmC_3-d(pTpG), AmC_3-d(pGpT), and AmC_3-d(pCpG) complexes display a positive ellipticity band around 440 nm. The similarity of the CD spectra of these complexes suggests that actinomycin acquires a similar environment in all cases. The CD spectrum of the AmC_3 + d(pGpC) complex shows an enhancement in the negative ellipticity band, which is also shifted to longer wavelengths (390 nm). Comparison of the spectra of AmC_3 + d(pGpC) with the above deoxydinucleotides reveals that the actinomycin environment in this complex is different from that in the other complexes.

Investigation of the Complexation of Ethidium Bromide with Some Deoxydinucleotides

The Ethidium Bromide-d(pCpG) Complex. Equilibrium Sedimentation. The quantity ψ in eq 2 is shown as a function of dinucleotide concentration in Figure 5. The dashed horizontal lines show the values expected for free ethidium and for the 2:1 complex of d(pCpG) with EBr. The close approach of the measured value to that expected for the 2:1 complex at high concentration is good evidence for that complex, as expected from earlier studies (Tsai et al., 1975; Krugh et al., 1975; Krugh and Reinhardt, 1975). The solid line is a theoretical curve calculated from the kinetic results (see below).

Melting Transitions. The concentration dependence of the melting temperature of the EBr + d(pCpG) complex is shown in Figure 6 for a series of experiments in which the ratio d(pCpG)/EBr was maintained at 2:1. The complex displays a monophasic melting profile, which is displaced toward higher T_m with increasing d(pCpG) concentration. The T_m values in Figure 6 were estimated from the temperature at which the absorbance rose by half the difference between the 0 °C and limiting high-temperature values. Similar T_m estimates were obtained from the inflection points in the sigmoid transition curves.

If one assumes that complex formation between EBr and

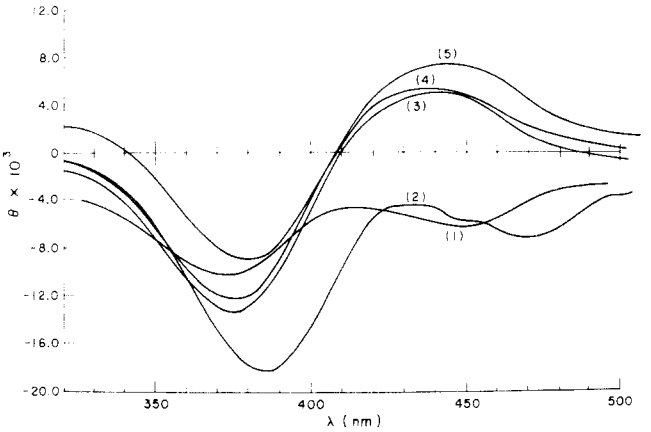

FIGURE 4: Circular dichroic ellipticity (degrees) as a function of wavelength for AmC_3-dinucleotides. T = 4 °C. (1) AmC_3 ($C_A°$ = 0.06 mM); (2) AmC_3-d(pGpC) ($C_N°$ = 0.584 mM); (3) AmC_3-d(pTpG) ($C_N°$ = 1.585 mM); (4) AmC_3-d(pGpT) ($C_N°$ = 1.38 mM); (5) AmC_3-d(pCpG) ($C_N°$ = 0.944 mM).

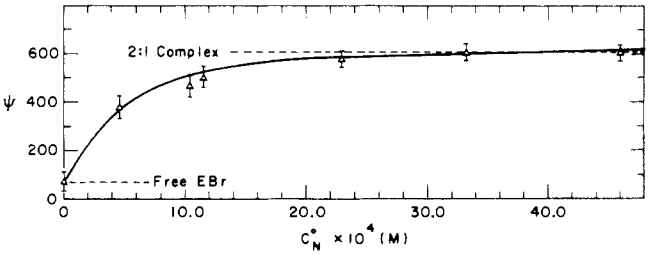

FIGURE 5: Variation of the quantity ψ, defined by eq 2a and 2b, with total dinucleotide concentration for the mixture of EBr with d(pCpG). The points (Δ) are experimental values calculated by eq 2b, and the line is a theoretical calculation using eq 2a and the binding equilibrium constants determined from the kinetic measurements (see below). λ = 465 nm, T = 8 °C, BPES buffer.

d(pCpG) is highly cooperative (this is just an approximation, since we will see later that the results of relaxation kinetics experiments indicate that formation of the EBr-2d(pCpG) complex is not a fully cooperative process), the formation of the complex can be described by the following thermodynamic equation:

$$\text{EBr} + 2\text{d(pCpG)} \rightleftarrows \text{complex}$$

with equilibrium constant

$$K = \frac{(\text{complex})}{\text{d(pCpG)}^2(\text{EBr})} \tag{4}$$

we define the following quantities: complex concentration = θC_0; d(pCpG) equilibrium concentration = $2C_0(1-\theta)$; EBr equilibrium concentration = $C_0(1-\theta)$ where C_0 is the initial EBr concentration and $2C_0$ is the initial d(pCpG) concentration. Insertion of these quantities in eq 4 and rearranging yields

$$KC_0^2 = \frac{\theta}{2(1-\theta)^3}$$

at the melting temperature (T_m), $\theta = \frac{1}{2}$ and $KC_0^2 = 2$. Taking logarithms and differentiating both sides gives:

$$\text{d ln } K = -2\text{d ln } C_0 \text{ at } T = T_m \tag{5}$$

With van't Hoff's equation we thus obtain

$$\frac{\Delta H°}{2R}\text{d}\left(\frac{1}{T_m}\right) = \text{d ln } C_0 \tag{6}$$

The variation of melting temperature with initial molar concentration of EBr is linear as predicted by eq 6, giving $\Delta H°$ = −27 kcal/mol for the enthalpy of EBr-2d(pCpG) complex formation. The equilibrium constant determined from this method is 1.3×10^7 M^{-2} at T = 7.5 °C.

Alternatively, ΔH can be found from the differential melting transition. The differential thermal profile of the EBr + d(pCpG) complex was determined from the relaxation amplitude following a temperature jump of ΔT = 4.6 °C at λ 465 nm. Making the assumption that complex formation is cooperative and using the analysis described by Gralla and Crothers (1973), one can derive the following relationship for enthalpy of complex formation

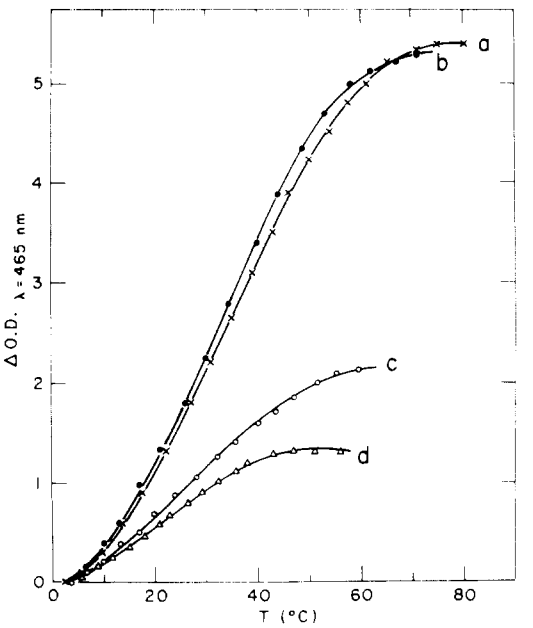

FIGURE 6: The melting transition profiles of the EBr + d(pCpG) complex monitored at 465 nm using a Cary 14 spectrophotometer, buffer 0.2 M Na^+ BPES (pH 6.9), d(pCpG) concentration: (a) 7 mM (T_m = 36 °C); (b) 6 mM (T_m = 33.5 °C); (c) 4.4 mM (T_m = 29 °C); (d) 2.77 mM (T_m = 23 °C). A d(pCpG)concentration/EBr concentration ratio of 2:1 was maintained in all melting experiments.

$$\Delta H = \frac{-5.09}{1/T_{1/2} - 1/T_{3/4}} \tag{7}$$

Using the values $T_{1/2}$ = 285 and $T_{3/4}$ = 299.2, we find $\Delta H°$ = −30.6 kcal from eq 7. K_{eq} determined by this method at T = 7.5 °C is 4.8×10^7 M^{-2}, roughly consistent with the value determined by the method involving the variation of T_m with concentration.

Kinetic Studies. Temperature-jump relaxation studies on the complex between EBr and d(pCpG) reveal one resolvable relaxation time in the range of a few hundreds of microseconds. About 25% of the optical change at 465 nm occurs within a few microseconds. Concentration dependences of the resolvable relaxation time at three different salt concentrations are shown in Figure 7. In 0.2 M Na^+ BPES buffer, $1/\tau$ has the same concentration dependence behavior except that the relaxation time is faster by a factor of about 1.4. In 1 M Na^+ BPES buffer, $1/\tau$ does not change with d(pCpG) concentration.

The Ethidium Bromide d(pGpC) Complex. The kinetic experiments for the EBr-d(pGpC) system show only one very

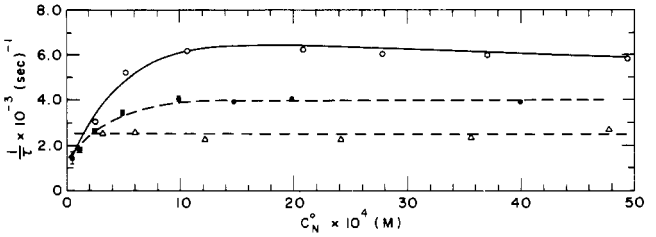

FIGURE 7: Variation of the reciprocal of relaxation times with total molar concentration of d(pCpG) for the d(pCpG) + EBr system: (●) in 0.2 M Na^+ BPES buffer; (○) in 0.05 M Na^+ BPES buffer; (△) in 1 M Na^+ BPES buffer. Total concentration of EBr = 0.169 mM, T = 7.1 °C. (- - -) The line of best fit calculated for the mechanism given in eq 8 using the rate constants summarized in Table I.

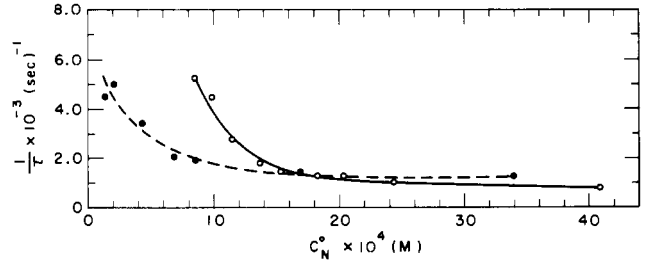

FIGURE 8: Variation of the reciprocal relaxation time with total molar concentration of dinucleotides. (●) (d(pCpA) + d(pTpG) mixture) + EBr, 0.2 M Na^+ BPES buffer, T = 7.1 °C, C_{EBr}° = 0.15 mM, λ = 465 nm; (○) d(pTpA) + EBr, 0.2 M Na^+ BPES buffer, T = 7.1 °C, C_{EBr}° = 0.178 mM, λ = 465 nm. (- - -) The line of best fit calculated for the mechanism given in eq 8 using the rate constants summarized in Table I.

fast relaxation time. The concentration dependence of this relaxation time displays a linear relationship of $1/\tau$ with concentration. The observed linear dependence of $1/\tau$ suggests that the EBr + d(pGpC) interaction is a simple bimolecular process:

$$\text{d(pGpC)} + \text{EBr} \underset{k_{21}}{\overset{k_{12}}{\rightleftharpoons}} \text{EBr-d(pGpC)} \qquad (8)$$

The kinetic equation for this mechanism is given by:

$$1/\tau = k_{12}[\text{EBr} + \text{d(pGpC)}] + k_{21} \qquad (9)$$

The constants $k_{12} = 2.2 \times 10^7\ M^{-1}\ s^{-1}$, $k_{21} = 10^4\ s^{-1}$, and $K = k_{12}/k_{21} = 2.2 \times 10^3\ M^{-1}$ were computed at 7.5 °C. (The low concentration of EBr allows the total nucleotide concentration to be substituted for $\overline{EBr} + \overline{d(pGpC)}$.)

Ethidium Bromide Binding to d(pCpA), d(pTpG), [d(pCpA) + d(pTpG)], and d(pTpA). We have investigated the relaxation kinetics of EBr-d(pCpA), EBr-d(pTpG), and EBr-[d(pCpA) + d(pTpG)]. It is observed that the interaction of EBr with d(pCpA) or d(pTpG) separately is a very fast process ($\tau < \mu s$) which cannot be measured by our temperature-jump method. The concentration dependence of the reciprocal of the relaxation time for EBr + [d(pCpA) + d(pTpG)] and EBr + d(pTpA) reveals a decrease with increasing concentration instead of an increase as observed for EBr + d(pCpG); the results are shown in Figure 8.

Discussion

Classes of Drug-Nucleotide Kinetic Behavior. We have observed three general types of kinetic behavior for interaction of dinucleotides with the drugs ethidium and actinomycin, as summarized in Table I. The general rule that emerges from Table I is that drugs which bind more than a single dinucleotide

TABLE I: Classes of Drug-Dinucleotide Kinetic Behavior.

1. Bimolecular:
   (a) Faster relaxation for interaction of Am with d(pTpG), d(pGpA), d(pApG), d(pGpG), d(pCpG), and D(pGpT)
   (b) Measurable relaxation for interaction of EBr with d(pGpC)
   (c) Bimolecular interaction of EBr with d(pCpA), d(pTpG), d(pTpA), and d(pCpG) inferred, but too fast to measure, or too small in amplitude to measure.
2. First-order rate limitation:
   (a) Slower relaxation for Am with d(pGpT), d(pTpG), d(pGpA), d(pApG), d(pGpG), and d(pCpG)
   (b) Measurable relaxation for interaction of EBr with d(pCpG), d(pTpA), and [d(pCpA) + d(pTpG)]
3. Termolecular: Am + d(pGpC)

show complex reaction kinetics, with the sole exception of actinomycin when binding cooperatively to 2 molecules of d(pGpC). All dinucleotides tested bind to actinomycin with a ratio of 2 dinucleotides per drug molecule (Davanloo and Crothers, 1976). In the case of ethidium, complex kinetics (first-order rate limitation) is seen only for dinucleotides of d(pPypPu) sequence, which are expected to form a double helix around an intercalated ethidium (Krugh and Reinhardt, 1975). Dinucleotides with other sequences, which are therefore not expected to form the 2:1 intercalated complex, show only bimolecular kinetics (case 1b in Table I) or an immeasureably fast relaxation (case 1c in Table I). We conclude that the first-order rate limitation is associated in some manner with attaching a second dinucleotide to the drug molecule.

The third-order kinetics observed for reaction of actinomycin with d(pGpC) is a special case. It is possible, even likely, that the reaction proceeds through a transient 1:1 complex intermediate

$$\text{Am} + \text{d(pGpC)} \rightleftarrows \text{Am-d(pGpC)}$$
$$\text{Am-d(pGpC)} + \text{d(pGpC)} \rightleftarrows \text{Am-[d(pGpC)]}_2$$

However, since no faster bimolecular relaxation could be observed, the concentration of the 1:1 intermediate must be small. It is not difficult to show that the two steps above will produce a single relaxation time which follows third-order kinetics if the concentration of the intermediate Am-d(pGpC) is negligible. The important contrast with all other 2:1 complexes studied is that no first-order rearrangement step intervenes to limit the reaction rate.

Possible Reaction Mechanisms. The results summarized in Table I present us with the problem of deciding on a reaction mechanism capable of explaining the observations. In order to predict a plateau in $1/\tau$ at high concentration, the mechanism must include at least one first-order step on the path to a 2:1 dinucleotide-drug complex. In principle, the first-order step could involve the uncomplexed molecule, the 1:1 complex, or the 2:1 complex. For example, in the reaction of ethidium with d(pCpG), we could propose any of the three possibilities:

$$\text{D} \rightleftarrows \text{D}^* + \text{E} \rightleftarrows \text{DE} + \text{D} \rightleftarrows \text{D}_2\text{E} \qquad \text{(a)}$$

$$\text{D} + \text{E} \rightleftarrows \text{DE} \rightleftarrows \text{DE}^* + \text{D} \rightleftarrows \text{D}_2\text{E} \qquad \text{(b)}$$

$$\text{D} + \text{E} \rightleftarrows \text{DE} + \text{D} \rightleftarrows \text{D}_2\text{E}^* \rightleftarrows \text{D}_2\text{E} \qquad \text{(c)}$$

In mechanism a, the first-order step involves the dinucleotide D, in b, the 1:1 complex DE, and in c, the 2:1 complex D_2E.

TABLE II: Values of the Rate Constants Which Were Used to Compute the Theoretical Curves (- - -) in Figures 7 and 8.[a]

System	k_{12} (M^{-1} s^{-1})	k_{21} (s^{-1})	k_{23} (s^{-1})	k_{32} (s^{-1})	k_{34} (M^{-1} s^{-1})	k_{43} (s^{-1})	K_{eq} (M^{-2})
EBr + d(pCpG) in 0.2 M Na^+ BPES buffer	7×10^6	7×10^2	4×10^3	(10^5)	(10^9)	(10^4)	4×10^7
EBr + d(pCpG) in 1 M Na^+ BPES buffer	(10^8)	(10^4)	3×10^3	(10^5)	(10^9)	10^3	3×10^8
EBr + [d(pCpA) + d(pTpG)]	10^7	5×10^3	1.5×10^3	(10^5)	(10^9)	(10^4)	3×10^6

[a] Values in parentheses affect the calculated results primarily through their ratios, as long as they are not substantially smaller than indicated.

The three mechanisms can be shown to differ in their predictions about the concentration dependence of the slow relaxation time under conditions such that the bimolecular steps are fast. Mechanism a predicts that $1/\tau$ should decrease as concentration increases, and mechanism c predicts an increase in $1/\tau$ as concentration increases. Only mechanism b can predict either an increase or a decrease depending on the rate constants. Since $1/\tau$ sometimes increases and sometimes decreases depending on the system and conditions, it is the only one of the three mechanisms capable of explaining all the results by itself.

An additional attractive feature of mechanism b is that one can see a simple physical basis for the rearrangement step. The complex of ethidium with single-stranded DNA certainly has a different structure from the double-stranded intercalation model, as indicated, for example, by the NMR measurements of Kreishman et al. (1971) or by the different spectral shift for the two structures (J. Bresloff and D. M. Crothers, unpublished data). Rearrangement of the single strand complex to a form able to accept another strand would account for the first order reaction step.

Calculation of Kinetic Parameters. Mechanism b contains six rate constants

$$E + D \underset{k_{21}}{\overset{k_{12}}{\rightleftharpoons}} ED \underset{k_{32}}{\overset{k_{23}}{\rightleftharpoons}} ED^* + D \underset{k_{43}}{\overset{k_{34}}{\rightleftharpoons}} ED_2 \qquad (10)$$

Since we were only able to measure one relaxation time in the ethidium–d(pCpG) system, we cannot expect to determine all six parameters by fitting the observed variation of $1/\tau$ with concentration. We can, however, show that the model is capable of predicting the results for all systems studied. Using standard methods (Eigen and DeMaeyer, 1963), we obtained and diagonalized the 3×3 matrix of kinetic coefficients corresponding to mechanism 10. The smallest eigenvalue λ_3 corresponds to the slowest observed relaxation time, $\lambda_3 = 1/\tau$. By insertion of trial values we found that a restricted range of values for some of the rate constants was required to fit the data, but that other constants needed simply to be faster than a minimum rate. Illustrative results are summarized in Table II and Figures 7 and 8 (dashed curves). We do not claim that other sets of values cannot be found which would also fit the kinetic data; our point is to show that the model is of sufficient complexity to accommodate the results. We could not find a simpler model that did so.

Circumstances are somewhat more propitious for determination of the rate constants for binding dinucleotides to actinomycin, since two relaxations are observable. We used the same mechanism as for the 1:2 ethidium–dinucleotide complexes.

$$A + D \underset{k_{21}}{\overset{k_{12}}{\rightleftharpoons}} AD \underset{k_{32}}{\overset{k_{23}}{\rightleftharpoons}} AD^* + D \underset{k_{43}}{\overset{k_{34}}{\rightleftharpoons}} AD_2$$

(This is a slight over-simplification, since actinomycin has two separate nucleotide binding sites, so formation of AD and conversion to its variant AD* must represent the sum of processes occurring at the two independent binding sites.) Figure 2 shows the calculated variation of the slower relaxation time with concentration of d(pApG) at constant actinomycin concentration (dashed curve) compared with the experimental measurements. The parameters used (see figure caption) also fit the linear variation of the faster relaxation time with dinucleotide concentration.

Comparison with Equilibrium Results. The kinetic parameters we report here are in satisfactory agreement with all the equilibrium information we had available or found in the course of our experiments. The individual cases are summarized here.

(1) Kinetic determination of the equilibrium constant for binding d(pGpC) to actinomycin (Figure 3) yields a value of $K = 7.6 \times 10^3$ M^{-1} for the square root of the termolecular association constant of the 2:1 complex, compared with 8.2×10^3 M^{-1} determined by the phase separation technique (Davanloo and Crothers, 1976).

(2) Kinetic analysis of the binding of d(pApG) to actinomycin yields values of $K = 2.1 \times 10^3$ M^{-1} for the sum of the binding constants for the two actinomycin sites, and $K = 1.0 \times 10^3$ M^{-1} for the square root of the termolecular association constant for the 2:1 complex (2 °C) compared with values of 1.5×10^3 and 1.5×10^3 M^{-1} determined from the phase separation technique (7 °C) (Davanloo and Crothers, 1976).

(3) The termolecular association constant calculated from the kinetic values for ethidium + 2d(pCpG) is 4×10^7 M^{-2}, compared with values ranging from 1.3×10^7 to 4.8×10^7 M^{-2} determined from the static (Figure 6) or temperature-jump melting curves. A more detailed test of the model is supplied by comparison with the equilibrium sedimentation results. Figure 5 shows the value of ψ predicted at various nucleotide concentrations using the equilibrium constants calculated from the kinetic constants (Table II, first line), compared with experimental data for EBr + d(pCpG) at 0.2 M Na^+ concentration.

Qualitative Conclusions

We found that all dinucleotides except d(pGpC) require a first-order step in the time range of a fraction of a millisecond in order to add a second nucleotide to the 1:1 actinomycin complex. This implies that the 1:1 AmD–d(pGpC) complex is unique: either it does not exist at all (which we consider unlikely) or its geometry is sufficiently close to that in the double helical complex that no slow rearrangement comparable to that in the other dinucleotide–actinomycin complexes is required.

For ethidium binding to dinucleotides, we found deviations from simple bimolecular kinetics only for systems containing

complementary d(pPypPu) sequences. We verified in detail for d(pCpG) that a 2:1 complex is formed, and proposed a reaction mechanism similar to that advanced for actinomycin, namely, that the first-order step is a rearrangement of the 1:1 complex. A possible structural basis for the first order step is implied by the conclusion of Kreishman et al. (1971) that the complex of ethidium with single stranded poly(U) differs in geometry from the complex with double helix. By this interpretation the rearrangement step is conversion of the 1:1 complex from the single-stranded form to an intermediate able to accept a second dinucleotide and complete the miniature double helix.

References

Bresloff, J. L., and Crothers, D. M. (1975), *J. Mol. Biol. 95,* 103.

Crothers, D. M. (1971), *Proced. Nucleic Acid Res. 2,* 369–388.

Davanloo, P., and Crothers, D. M. (1976), *Biochemistry* (in press).

Eigen, M., and DeMaeyer, L. (1963), *Tech. Org. Chem. 8* (2), 896–1054.

Elliott, W. H. (1963), *Biochem. J. 86,* 562.

Fuller, W., and Waring, M. J. (1964), *Ber. Bunseng. 68,* 805.

Gralla, J., and Crothers, D. M. (1973), *J. Mol. Biol. 78,* 301.

Henderson, J. F. (1963), *Cancer Res. 23,* 491.

Kersten, W., Kersten, H., and Raven, H. M. (1960), *Nature (London) 187,* 60.

Kirk, J. (1960), *Biochim. Biophys. Acta 42,* 167.

Kreishman, G. P., Chan, S. I., and Bauer, W. (1971), *J. Mol. Biol. 61,* 45.

Krugh, T. R. (1972), *Proc. Natl. Acad. Sci. U.S.A. 69,* 1911.

Krugh, T. R., and Neely, J. W. (1973a), *Biochemistry 12,* 1775.

Krugh, T. R., and Neely, J. W. (1973b), *Biochemistry 12,* 4418.

Krugh, T. R., and Reinhardt, G. C. (1975), *J. Mol. Biol. 97,* 133.

Krugh, T. R., Wittlin, F. N., and Cramer, S. P. (1975), *Biopolymers 14,* 197.

Lerman, L. S. (1961), *J. Mol. Biol. 3,* 18.

Müller, W., and Crothers, D. M. (1968), *J. Mol. Biol. 35,* 251.

Müller, W., and Spatz, H. Ch. (1965), *Z. Naturforsch. B 20,* 842.

Schara, R., and Müller, W. (1972), *Eur. J. Biochem. 29,* 210.

Sobell, H. M., and Jain, S. C. (1971), *Nature, (London) (New Biol.) 231,* 200.

Sobell, H. M., and Jain, S. C. (1972), *J. Mol. Biol. 68,* 21.

Tanford, C. (1961), Physical Chemistry of Macromolecules, New York, N.Y., Wiley, p 269.

Tsai, C. C., Jain, S. C., and Sobell, H. M. (1975), *Proc. Natl. Acad. Sci. U.S.A. 72,* 628.

Wang, J. C. (1971), *Biochim. Biophys. Acta 232,* 246.

Waring, M. J. (1964), *Biochim. Biophys. Acta 87,* 358.

Waring, M. J. (1970), *J. Mol. Biol. 54,* 247.

Studies on DNA α-Polymerase of Mouse Myeloma: Partial Purification and Comparison of Three Molecular Forms of the Enzyme†

A. Matsukage,‡ M. Sivarajan, and S. H. Wilson*

ABSTRACT: Activity of DNA α-polymerase in extracts from MOPC-104E was not associated with a single protein molecule, but with several molecular species that differed in isoelectric point. The three most abundant of these enzyme species were first separated from other DNA polymerases and then resolved from each other by repeated chromatography on diethylaminoethylcellulose columns. Next, with the use of glycerol gradient centrifugation and DNA-cellulose column chromatography, the three species were further purified to a state representing more than 5000-fold purification over the crude extract. These three highly purified enzyme species exhibited very similar catalytic properties, and the main activity of each species sedimented at the same rate (6–7S) in glycerol gradients containing 0.5 M KCl. Analysis of the polypeptide content of each species revealed that polypeptides of about 150 000 and 60 000 daltons cofractionated with the DNA polymerase activity. The multiple α-polymerase species did not appear to result from in vitro proteolytic cleavage, since multiple species were observed in extracts prepared under several different types of conditions, including the presence of the protease inhibitors, phenylmethanesulfonyl fluoride, or trasylol. The three species were recovered in about the same relative amounts from both the nuclear and cytoplasmic fractions of MOPC-104E, and it appeared that multiple species of α-polymerase were also present in extracts from fetal bovine liver.

The purification of DNA α-polymerase has been hampered both by the instability of the enzyme (Bollum et al., 1974) and by its molecular heterogeneity, which has now been observed in extracts from several mammalian cell types (Chang et al., 1973; Momparler et al., 1973; Ove et al., 1973; Holmes and Johnston, 1973; Yoshida et al., 1974; Holmes et al., 1974; Matsukage et al., 1974; Bollum, 1975; Hachmann and Lezius, 1975). Significant molecular heterogeneity, however, was not observed in some other mammalian tissues (Smith et al., 1975;

† From the Laboratory of Biochemistry, National Cancer Institute, National Institutes of Health, Bethesda, Maryland 20014. *Received April 14, 1976.*

‡ Present address: Laboratory of Biochemistry, Aichi Cancer Center, Research Institute, Chikusa-Ku, Nagoya, Japan.